Thermalization of quark gluon matter

Bin Wu
IGFAE, Universidade de Santiago de Compostela

Lecture 1: fundamentals

- 1. Introduction to real-time dynamics in QCD
- 2. Parton saturation, classical fields and quasi-particles

Lecture 2: applicaitons

- 3. Thermalization of the quark-gluon plasma
- 4. Perspective: flow in small systems

QCD and Heavy Ion Collision Physics Summer School, Fudan U., 08/23/2024

1.1 Recap of QCD

- The QCD Lagrangian

$$\mathcal{L} = -\frac{1}{4} F^a_{\mu\nu} F^{a\mu\nu} + \sum_f \bar{q}_f (iD_\mu \gamma^\mu - m_f) q_f \tag{1}$$

where $D_\mu = \partial_\mu - igA_\mu$ and $F_{\mu\nu} = \partial_\mu A_\nu - \partial_\nu A_\mu - ig[A_\mu, A_\nu]$ with $A_\mu \equiv A^a_\mu t^a$ and t^a the $SU(N_C)$ generators in the fundamental representation. Here, $N_c = 3$ in the real world.

- The color matrices obey

$$\begin{aligned} [t^a, t^b] &= if^{abc} t^c, \qquad \mathrm{Tr}[t^a t^b] = \frac{\delta^{ab}}{2}, \\ f^{abc} f^{abd} &= C_A \delta^{cd}, \qquad (t^a t^a)_{bc} = C_F \delta_{bc}, \end{aligned} \tag{2}$$

with $C_A \equiv N_c$, $\quad C_F \equiv \frac{N_c^2 - 1}{2N_c}$.

In principle, all the properties of the strong interaction can be derived from $\mathcal{L}$.

• QCD is renormalizable and all ultraviolet (UV) divergences can be removed by redefining the coupling constant, quark masses and the field strengths. This renormalization procedure introduces some renormalization scale μ.

• The running coupling: $\alpha_s(\mu) \equiv \frac{g^2(\mu)}{4\pi}$

$$\frac{d\alpha_s(\mu)}{d\ln\mu} = \beta(\alpha_s(\mu)), \quad \beta(\alpha_s) = -2\alpha_s \sum_{n=0}^{\infty} \beta_n \left(\frac{\alpha_s}{4\pi}\right)^{n+1} \tag{3}$$

with $\beta_0 \equiv \frac{11}{3}C_A - \frac{2}{3}N_f$, $\beta_1 = \frac{34}{3}C_A^2 - \frac{10}{3}C_A N_f - 2C_F N_f$ etc. and N_f the number of active quarks.

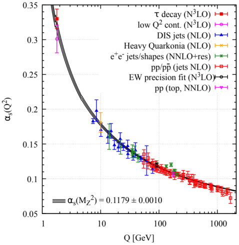

Particle Data Group collaboration, Review of Particle Physics, PTEP 2022 (2022) 083C01.

• QCD shows asymptotic freedom at short distance: $\alpha_s(Q) \to 0$ as $Q \to \infty$. Therefore, we can safely use pertrubation theory at large Q.

• QCD becomes nonperturbative at long distances, which is characterized by a low momentum scale: **the Lambda parameter** defined as

$$\ln \frac{Q}{\Lambda_{QCD}} = -\int_{\alpha_s(Q)}^{\infty} \frac{d\alpha_s}{\beta(\alpha_s)} \quad (4)$$

That is, $\alpha_s(Q) \to \infty$ as $Q \to \Lambda_{QCD}$. At one loop, one has

$$\ln \frac{Q}{\Lambda_{QCD}} = \frac{2\pi}{\beta_0 \alpha_s(Q)}. \quad (5)$$

$\Lambda_{QCD} \sim 200$ MeV $\approx 1/$(proton size) sets the scale of nonperturbative physics although its exact value depends on the renormalization scheme when β is calculated up to high orders in α_s.

$\alpha_s(Q \to \Lambda_{QCD}) \to \infty$ only implies the breaking down of perturbation theory.

• A parton with p^μ can be reliably described by perturbative QCD when its virtuality $|p^2| \gg \Lambda_{QCD}^2$.

1.2 Real-time dynamics in heavy-ion collisions

- Focus on **bulk matter**: 99% of the produced particles excluding hard probes

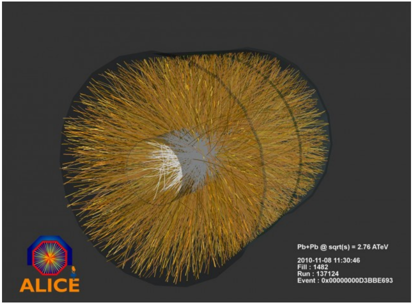

Trajectories of charged hadrons in PbPb collisions

Estimates for bulk matter:

In pp collisions at the LHC

$$\frac{dN_{pp}}{d\eta d\phi} \sim 1, \quad \langle p_T \rangle \sim 1 \text{ GeV at } \eta \sim 0$$

In central AA collisions (e.g. PbPb)

$$\frac{dN_{AA}}{d\eta} \sim A\frac{dN_{pp}}{d\eta} \sim 10^3 \text{ at } \eta \sim 0$$

See Prof. Ollitrault's argument in this school.

$$\varepsilon(t = 1\ fm/c) \sim \langle p_T \rangle \frac{dN_{AA}}{d\eta}\frac{1}{tR^2} \sim 10 GeV/fm^3.$$

$\varepsilon(t = 1\ fm/c) = 14\ GeV/fm^3$ based on measurement in CMS: Phys. Rev. Lett. **109**, 152303 (2012) [arXiv:1205.2488 [nucl-ex]]

- QGP in thermal equilibrium (with $\mu_B = 0$) is viable to first-principle calculation in QCD:

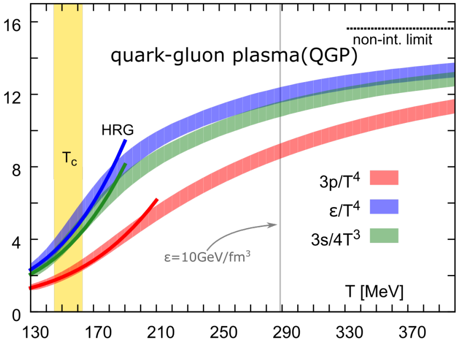

Lattice QCD: Phys. Rev. D **90**, 094503 (2014) [arXiv:1407.6387 [hep-lat]].

- For example, the partion function $Z_\beta = \int D\Phi_f e^{-S_E[\Phi_f]}$ with Φ_f standing for quarks and gluon fields: numerically easier to evaluate as long as $S_E \geq 0$.

Thermalization: how QCD matter evolves into QGP in thermal equilibrium.

• Bulk matter $\neq$ QGP in thermal equilibrium

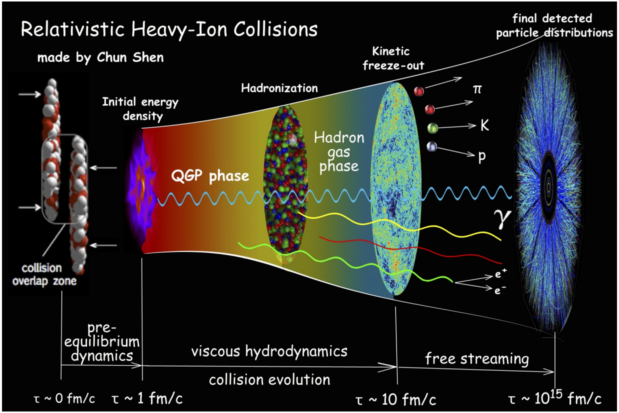

• Preequilibrium dynamics in the nonperturbative regime is yet to be addressed from QCD first principles due to the sign problem. The heavy-ion community has invented a terminology for this issue: **hydrodynamization**.

For a comprehensive review, see P. Romatschke and U. Romatschke, Cambridge University Press, 2019, [arXiv:1712.05815 [nucl-th]].

1.3 Tools for studying real-time dynamics in QFT

• **The sign problem:** the evaluation of path integral for real-time dynamics in general involves highly oscillatory functions. It is not known yet how it can be overcome (in lattice QCD).

$$\underbrace{Z_\beta = \int D\Phi_f e^{-S_E[\Phi_f]}}_{\text{imaginary time}} \to \underbrace{Z = \int D\Phi_f e^{iS[\Phi_f]}}_{\text{real time}}$$

For preequilibrium dynamics beyond the perturbative regime:

• 1 CFT model - AdS/CFT: thermalization = blackhole formation in AdS_5

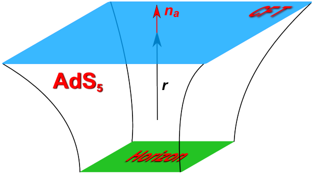

For $\lambda \equiv g^2 N_c \gg 1$ and $N_c \to \infty$, the thermalization time $\sim 1/T$.

See Prof. Hou's lecture 4 or J. Casalderrey-Solana, H. Liu, D. Mateos, K. Rajagopal, U. A. Wiedemann, [arXiv:1101.0618 [hep-th]].

- 2 Quantum Computing for QCD? Promising but not feasible in the near term
  - Rapid development in quantum processors

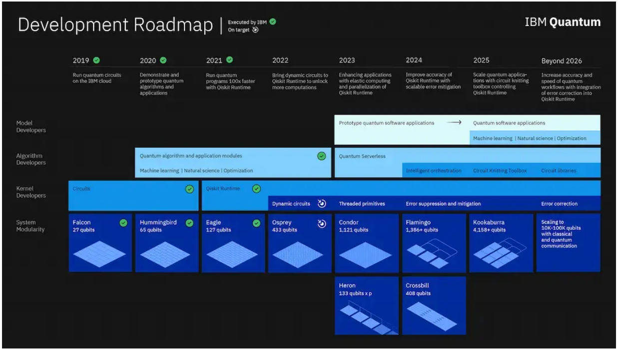

  - Currently, we are in the Noisy Intermediate-Scale quantum (NISQ) era:
    - Noisy: sensitive to their environment, prone to quantum decoherence
    - Intermediate-Scale: quantum processors containing up to 1000 qubits

J. Preskill, Quantum **2** (2018), 79 [arXiv:1801.00862 [quant-ph]].

Let us first explore the weak-coupling/high-energy limit!

2.1 PDFs and parton saturation

- The DGLAP equations: the evolution of PDFs is governed by the $1 \to 2$ splitting. For the gluon distribution function, one has

$$\frac{d}{d\ln\mu} f_{g/h}(x,\mu) = \frac{\alpha_s(\mu)}{\pi}\int_x^1 \frac{dz}{z}\Big\{P_{g\leftarrow q}(z)\sum_f [f_{q_f/h}(x/z,\mu) + f_{\bar{q}_f/h}(x/z,\mu)] + P_{g\leftarrow g}(z) f_{g/h}(x/z,\mu)\Big\} \quad (6)$$

- It leads to a rapid growth in the gluon distribution at small x. In the double log approximation, one has

$$xG(x,Q) \equiv xf_g(x,Q) \sim \frac{1}{2\sqrt{\pi}}\left[\frac{\bar{\alpha}\ln(Q/\Lambda)}{\ln^3(1/x)}\right]^{\frac{1}{4}} \exp\left\{2\left[\bar{\alpha}\ln\left(\frac{Q}{\Lambda}\right)\ln\left(\frac{1}{x}\right)\right]^{\frac{1}{2}}\right\} \text{ with } \bar{\alpha} \equiv \frac{2\alpha_s C_A}{\pi}.$$

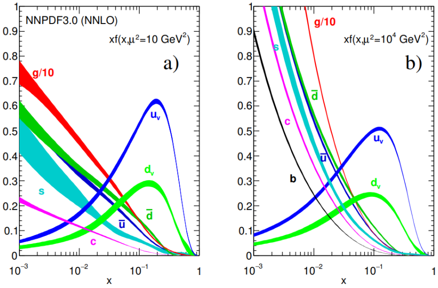

• The DGLAP equations are expected to break down at small x. One would expect that the recombination $2 \to 1$ processes become important too when $xG \gg 1$, leading to **gluon saturation**.

• Color-Class-Condensate (CGC): an EFT for quantitatively studying parton saturation. *F. Gelis, et. al., Ann. Rev. Nucl. Part. Sci.* **60**, *463 (2010)*

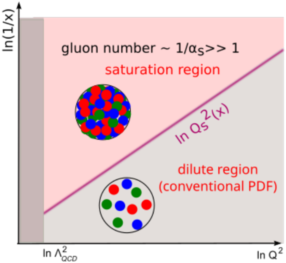

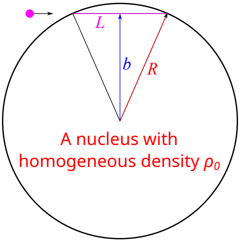

• **The saturbation momentum** (for a spherical nucleus):

$$Q_s^2 = \frac{8\pi^2 \alpha_s N_c}{N_c^2 - 1} \sqrt{R^2 - b^2} \rho_0 x G \sim (2-4)\text{GeV}^2 \text{ at the LHC.}$$

In heavy nuclei, (saturated) gluons have a typical momentum $\sim Q_s$.

A. H. Mueller, [arXiv:hep-ph/0111244 [hep-ph]].

- Due to the rapid growth in xG at small x, the number of gluons freed in the very early stage of the collision is large. In CGC,

$$xG \sim 1/\alpha_s \Leftrightarrow A^\mu \sim 1/g$$

. Let us focus on the limit with $Q_s \gg \Lambda_{QCD}$ (and hence $\alpha_s \ll 1$) below.

- After the collision, one may expect

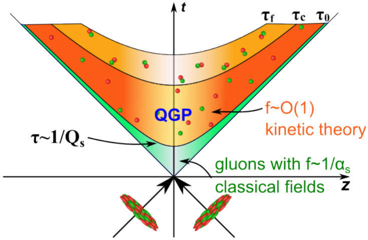

1. At very early stages, the gluon density is high. Classical field applies.
2. At later stages, the gluon density becomes dilute. Kinetic theory applies.

In each case, one needs only to sum over a certain subgroup of diagrams of the full theory (and one can forget about the sign problem)

2.2 The Schwinger-Keldysh (KS) formalism

- The evolution operator from $|\phi_0\rangle$ at $t = 0$ to $|\phi_t\rangle$ at t

$$U(t) \equiv \int_{\phi(0)\,=\,\phi_0,\ \phi(t)\,=\,\phi_t} D\phi\, e^{iS[\phi]}$$

with t integrated over [0, t] in S and ϕ standing for all the fields in a QFT.

- Given $\hat{\rho}(t)$ at $t = 0$, one has, for any observable $\hat{O}$, e.g., $\hat{T}^{\mu\nu}$

$$\langle \hat{O}(t)\rangle = \mathrm{Tr}\left[\hat{O}\hat{\rho}(t)\right] = \mathrm{Tr}\left[\hat{O}U(t)\hat{\rho}(0)U(t)^{\dagger}\right]$$

SK contour: 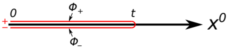

$$= \int d\phi_0 d\phi_t \int_{\substack{\phi_\pm(0)\,=\,\phi_0 \\ \phi_\pm(t)\,=\,\phi_t}} D\phi_+ D\phi_-\, \hat{O}[\phi(t)] e^{iS[\phi_+]} \langle \phi_{+0}|\hat{\rho}(0)|\phi_{-0}\rangle e^{-iS[\phi_-]}$$

$$= \int d\phi_0 d\phi_t \int_{\substack{\phi_\pm(0)\,=\,\phi_0 \\ \phi_\pm(t)\,=\,\phi_t}} D\phi_+ D\phi_-\, e^{iS[\phi_+]-iS[\phi_-]} \hat{O}[\phi(t)] \langle \phi_{+0}|\hat{\rho}(0)|\phi_{-0}\rangle \qquad (7)$$

It can be viewed as a QFT with a double number of fields.

- We define $\phi_1 = \phi_+ - \phi_-$ and $\phi_2 = (\phi_+ + \phi_-)/2$.
- In QCD, the interaction Lagrangian takes the form

$$\mathcal{L}_I \equiv \mathcal{L}_I(\phi_+) - \mathcal{L}_I(\phi_-) = -gf^{abc}\partial_\mu \eta^a_\nu A^{b\mu} A^{c\nu} - gf^{abc}\partial_\mu A^a_\nu \eta^{b\mu} A^{c\nu} - gf^{abc}\partial_\mu A^a_\nu A^{b\mu}\eta^{c\nu}$$
$$- \frac{g}{4} f^{abc}\partial_\mu \eta^a_\nu \eta^{b\mu}\eta^{c\nu} - g^2 f^{abc} f^{ade} \eta^b_\mu A^c_\nu A^{c\mu} A^{d\nu} - \frac{g^2}{4} f^{abc} f^{ade}\eta^b_\mu \eta^c_\nu \eta^{c\mu} A^{d\nu}$$
$$+ g\bar{q}_1 A q_2 + g\bar{q}_2 A q_1 + g\bar{q}_2 \eta q_2 + \frac{g}{4}\bar{q}_1 \eta q_1 \qquad (8)$$

with $A^\mu \equiv A^\mu_2$ and $\eta^\mu \equiv A^\mu_1$.

- The free propagators (in the lightcone gauge)

$$S^{(0)}(k,m) = (k+m)\, G^{(0)}(k,m),$$
$$G^{(0)\mu,b\nu}(k) = \left(-g^{\mu\nu} + \frac{k^\mu n^\nu + k^\nu n^\mu}{n\cdot k}\right) G^{(0)}(k,0). \qquad (9)$$

with the free propagator for ϕ given by

$$G^{(0)}(k,m) = \begin{pmatrix} 0 & \frac{i}{p^2-m^2-ip^0\epsilon} \\ \frac{i}{p^2-m^2+ip^0\epsilon} & \pi\delta(p^2-m^2) \end{pmatrix} \equiv \begin{pmatrix} 0 & G_A(p,m) \\ G_R(p,m) & G_S(p,m) \end{pmatrix}.$$

BW and Y. V. Kovchegov, JHEP **03** (2018), 158 [arXiv:1709.02866 [hep-ph]].

Now, one only needs to evalute the path integral on the SK contour.

2.3 The classical statistical approximation (CSA)

- For simplicity, let us take the ϕ^4 theory:

$$\mathcal{L} \equiv \mathcal{L}(\phi_+) - \mathcal{L}(\phi_-) = -\phi_1[(\Box + m^2)\phi_2 + \underbrace{g^2/6\phi_2^3}_{\text{classical vertex}}] - \underbrace{g^2/24\phi_1^3\phi_2}_{\text{quantum vertex}} \quad (10)$$

- For an observable $\hat{O}$, one has

$$\langle \hat{O}(t) \rangle = \int d\phi_t d\phi_0 \underbrace{\int d\sigma_0 e^{-i\hbar\sigma_0\pi_0} \langle \phi_0 + \sigma_0/2 | \hat{\rho}(0) | \phi_0 - \sigma_0/2 \rangle}_{\rho_W[\phi_0,\pi_0] \text{ with } \pi_0 = \dot{\phi}_0} \hat{O}[\phi_t] \quad (11)$$

$$\times \int_{\substack{\phi_1(0)=\sigma_0,\ \phi_1(t)=0 \\ \phi_2(0)=\phi_0,\ \phi_2(t)=\phi_t}} D\phi_1 D\phi_2 e^{-i\int_0^t dx^0 \int d^3\vec{x}\{\phi_1[(\Box+m^2)\phi_2 + \underbrace{g^2/6\phi_2^3}_{\text{classical vertex}}] + \underbrace{g^2/24\phi_1^3\phi_2}_{\text{quantum vertex}}\}}.$$

- When $\phi_2 \sim 1/g$, the quantum vertex $g^2/24\phi_1^3\phi_2$ only gives arise to subleading corrections. In classical field approximation, this vertex is neglected.

- As a result, one arrives at **the classical statistical approximation(CSA)**:

$$\langle \hat{O}(t)\rangle = \int d\phi_0 d\pi_0 \rho_W[\phi_0, \pi_0]\hat{O}[\phi_{cl}(t)].$$

where

$$\Box\phi_{cl} + \frac{g^2}{6}\phi_{cl}^3 = 0 \text{ with } \phi_{cl}(0) = \phi_0, \dot{\phi}_{cl}(0) = \pi_0. \tag{12}$$

That is, one only needs to solve the equation of motion of the classical fields, which are then average over some initial distribution described by the Wigner distribution ρ_W. (See Prof. Teaney's lectures in this school!)

- Proof: dropping the quantum vertex $-g^2/24\phi_1^3\phi_2$

$$\langle \hat{O}(t)\rangle = \int d\phi_t d\phi_0 \int d\sigma_0 e^{-i\hbar\sigma_0\pi_0}\langle\phi_0 + \sigma_0/2|\hat{\rho}(0)|\phi_0 - \sigma_0/2\rangle \hat{O}[\phi_t]$$

$$\times \int_{\substack{\phi_1(0)=\sigma_0,\ \phi_1(t)=0 \\ \phi_2(0)=\phi_0,\ \phi_2(t)=\phi_t}} D\phi_2 \underbrace{D\phi_1 e^{-i\int_0^t dx^0 \int d^3\vec{x}\left[\phi_1\left(\Box\phi_2 + g^2/6\phi_2^3\right)\right]}}_{\delta\left[\Box\phi_2 + g^2 6\phi_2^3\right]}. \tag{13}$$

The Jacobian from the δ functional replaces the boundary condition $\phi_2(t) = \phi_t$ with $\dot{\phi}_2(0) = \pi_0$ to yield the CSA formula.

A. H. Mueller and D. T. Son, Phys. Lett. B **582**, 279 (2004) [hep-ph/0212198].

S. Jeon, Phys. Rev. C **72** (2005), 014907 [arXiv:hep-ph/0412121 [hep-ph]].

• However, we found that CSA is nonrenormalizable. That is, a QFT with $\mathcal{L} = -\phi_1[(\Box + m^2)\phi_2 + g^2/6\phi_2^3]$ needs (nonlocal) counterterms that are not in $\mathcal{L}$ to cancel UV divergences.

T. Epelbaum, F. Gelis and BW, Phys. Rev. D **90** (2014) no.6, 065029 [arXiv:1402.0115 [hep-ph]].

• Implications: the late-time behavior in classical field simulations will eventually depend on UV cutoff Λ_{UV}/lattice spacing.

• For example, if the thermal distribution for the Boltzmann equation under the classical approximation is given by

$$f = \frac{T}{p} \Rightarrow T \propto \epsilon/\Lambda_{UV}^3 \tag{14}$$

for massless scalars due to (ϵ) energy conservation.

Note its difference from the Boltzmann distribution!

• Conclusion: One can not use classical field simulations to describe thermalization.

2.4 Kinetic theory vs QFT

- Kinetic theory is suited for studying thermalization. It has been widely used for studying thermalization/hydrodynamization.

For simplicity, let us first neglect quarks:

- The Dyson-Schwinger equation resums over one-particle-irreducible (1PI) self-energies. The 1PI diagrams correspond to some single scattering process. This equation iterates 1PI self-energies, effectively taking into account effects of a number of such scatterings.

$$\Box^{\mu}_{x\ \rho} G^{a\rho,b\nu}_{22}(x,y) = \int d^4z\ \Pi^{a\mu}_{11\ c\rho}(x, X+z) G^{c\rho,b\nu}_{12}(X+z,y) + \int d^4z\ \Pi^{a\mu}_{12\ c\rho}(x, X+z) G^{c\rho,b\nu}_{22}(X+z,y), \tag{15}$$

$$\Box^{\mu}_{y\ \rho} G^{b\nu,a\rho}_{22}(x,y) = \int d^4z\ G^{b\nu,c\rho}_{21}(x, X+z) \Pi_{11\,c\rho}{}^{a\mu}(X+z,y) + \int d^4z\ G^{b\nu,c\rho}_{22}(x, X+z) \Pi_{21\,c\rho}{}^{a\mu}(X+z,y), \tag{16}$$

with $X^{\mu} \equiv \frac{x^{\mu}+y^{\nu}}{2}$ and Π's being self-energies.

- From the Dyson-Schwinger equation, after some approximation one has

$$\left[-2ig_\rho^\mu p\cdot\partial_X + ip^\mu\partial_{X\rho} + ip_\rho\partial_X^\mu\right] G_{22}^{a\rho,b\nu} = \left[\Pi_{12}^{a\mu}{}_{c\rho} - \Pi_{21\,c\rho}{}^{a\mu}\right] G_{22}^{c\rho,b\nu} + \Pi_{11}^{a\mu}{}_{c\rho}\left[G_{12}^{c\rho,b\nu} - G_{21}^{b\nu,c\rho}\right]. \qquad (17)$$

where G stands for $G^{a\mu,b\nu}(X,p) \equiv \int d^4x e^{ip\cdot x} G^{a\mu,b\nu}\left(X+\frac{x}{2}, X-\frac{x}{2}\right)$.

- The quasiparticle approximation:

$$G_{21}^{a\mu,b\nu}(X,p) = \delta^{ab}\left(-g^{\mu\nu} + \frac{p^\mu n^\nu + p^\nu n^\mu}{n\cdot p}\right) G_R(p),$$

$$G_{12}^{a\mu,b\nu}(X,p) = \delta^{ab}\left(-g^{\mu\nu} + \frac{p^\mu n^\nu + p^\nu n^\mu}{n\cdot p}\right) G_A(p),$$

$$G_{22}^{a\mu,b\nu}(X,p) = 2\pi\delta^{ab}\left(-g^{\mu\nu} + \frac{p^\mu n^\nu + p^\nu n^\mu}{n\cdot p}\right)\left[f(X,p)+\frac{1}{2}\right]\delta(p^2) \qquad (18)$$

For more details, see Appendix B in BW and Y. V. Kovchegov, JHEP **03** (2018), 158 [arXiv:1709.02866 [hep-ph]].

- Diagrams for $\Pi_{11}^{a\mu,b\nu}$:

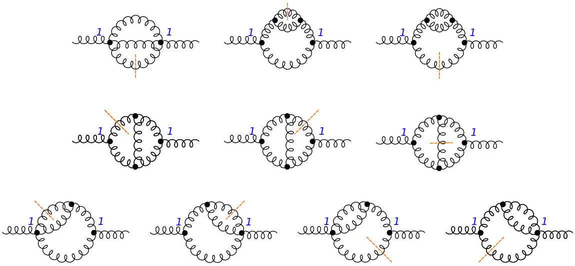

- Diagrams for $\Pi_{21}^{a\mu,b\nu}$:

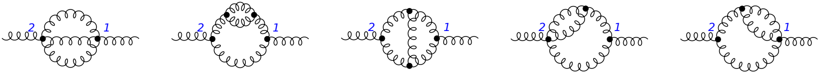

Internal propagators are given by those in the quasiparticle approximation.

• After some algebra, one obtains the Boltzmann equation for gluons

$$p\cdot\partial f = \frac{1}{4}\int_{p_1,p_2,p_3}(2\pi)^4\delta(p+p_1-p_2-p_3)\overline{|M|^2} \times [f_2 f_3(f+1)(f_1+1) - f f_1(f_2+1)(f_3+1)] \quad (19)$$

with $\overline{|M|^2} = 8N_c^2 g^4\left(3-\frac{tu}{s^2}-\frac{su}{t^2}-\frac{st}{u^2}\right)$.

The derivation can be generalized to include inelastic processes.

• Note QFT is richer but more complicated. For example, our fixed-order calculations yield

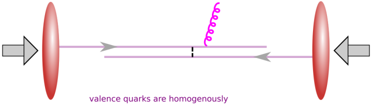

$$G_{22}^{a\mu,b\nu}(X,p) \propto \delta^{ab}\frac{\cos\left(2\tau\sinh(y-\eta)\sqrt{p^2}\right)}{\sqrt{2p^-p^+p^2}}\sum_{\lambda=\pm}\epsilon_\lambda^\mu(p)\epsilon_\lambda^{*\nu}(p).$$

with $\eta \equiv \frac{1}{2}\ln\left(\frac{x^+}{x^-}\right)$ and $y \equiv \frac{1}{2}\ln\left(\frac{p^+}{p^-}\right)$.

2.5 The QCD Boltzmann equation

• The QCD Boltzmann equation at leading order includes both elastic and inelastic kernels:

$$(\partial_t + \mathrm{v} \cdot \nabla_{\mathrm{x}}) f^a = C^a_{2\leftrightarrow 2}[f] + C^a_{1\leftrightarrow 2}[f] , \quad f^a = \{f^g, f^q, f^{\bar{q}}\} \tag{20}$$

R. Baier, A. H. Mueller, D. Schiff and D. T. Son, Phys. Lett. B **502** (2001), 51-58 [arXiv:hep-ph/0009237 [hep-ph]].

Effective Kinetic Theory (EKT): P. B. Arnold, G. D. Moore and L. G. Yaffe, JHEP **01** (2003), 030 [arXiv:hep-ph/0209353 [hep-ph]].

• The Boltzmann equation in diffusion approximation (BEDA): The $2 \leftrightarrow 2$ processes are dominated by small angle scattering (t or $u \to 0$), yielding logarithmic terms in the kernel.

• Keeping only the logarithmic terms, the $2 \leftrightarrow 2$ collision kernel can be expressed in a Fokker-Planck form plus an additional source term.

$$C^a_{2\leftrightarrow 2} = \frac{1}{4} \hat{q}_a(t) \nabla_{\boldsymbol{p}} \cdot \left[\nabla_{\boldsymbol{p}} f^a + \frac{\mathrm{v}}{T^*(t)} f^a (1 + \epsilon_a f^a) \right] + \mathcal{S}_a \tag{21}$$

where $\epsilon_a = 1$ for bosons and $\epsilon_a = -1$ for fermions, and $T_*(t) \equiv \frac{\hat{q}_A}{\alpha_s N_c \mathcal{L} m_D^2}$ with $\mathcal{L} \equiv \ln \frac{\langle p_t^2 \rangle}{m_D^2}$, and $\langle p_t^2 \rangle = \frac{2}{3} \langle p^2 \rangle$ for isotropic systems.

J. P. Blaizot, BW and L. Yan, Nucl. Phys. A **930** (2014), 139-162 [arXiv:1402.5049 [hep-ph]].

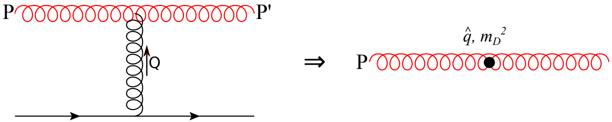

- The screening mass squared is defined as

$$m_D^2 = m_{D,g}^2 + m_{D,q}^2 + m_{D,\bar{q}}^2 \equiv 8\pi\alpha_s \int \frac{d^3\boldsymbol{p}}{(2\pi)^3} \frac{1}{|\boldsymbol{p}|} \left[2N_c f^g + \sum_{i=1}^{N_f} (f^{q^i} + f^{\bar{q}^i}) \right]$$

with $m_{D,a}^2$ standing for the contribution from parton a.

- The jet quenching parameter for species a is defined as $\hat{q}_a = C_a \hat{\bar{q}}$, and

$$\hat{\bar{q}} \equiv 4\pi\alpha_s^2 \mathcal{L} \int \frac{d^3\boldsymbol{p}}{(2\pi)^3} \left\{ 2N_c f^g (1 + f^g) + \sum_{i=1}^{N_f} [f^{q^i}(1 - f^{q^i}) + f^{\bar{q}^i}(1 - f^{\bar{q}^i})] \right\}$$

where $C_a = \{C_A = N_c, C_F\}$ respectively for g and $q^i/\bar{q}^i$. See Prof. Wang's lectures!

- Interpretation of $\hat{q}$: transverse momentum broadening per unit path length. If the time dependence of $\hat{q}$ is negligible, one has

$$\langle p_\perp^2 \rangle = \hat{q} t$$

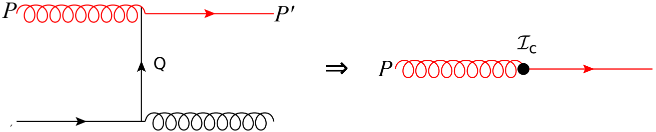

- Let extend the source terms for each quark flavor i,

$$\mathcal{S}_{q^i} = \frac{2\pi\alpha_s^2 C_F^2 \mathcal{L}}{p}\left[\mathcal{I}_c^i f^g(1-f^{q^i}) - \bar{\mathcal{I}}_c^i f^{q^i}(1+f^g)\right],$$

$$\mathcal{S}_{\bar{q}^i} = \frac{2\pi\alpha_s^2 C_F^2 \mathcal{L}}{p}\left[\bar{\mathcal{I}}_c^i f^g(1-f^{\bar{q}^i}) - \mathcal{I}_c^i f^{\bar{q}^i}(1+f^g)\right],$$

$$\mathcal{S}_g = -\frac{1}{2C_F}\sum_{i=1}^{N_f}(\mathcal{S}_{q^i} + \mathcal{S}_{\bar{q}^i}), \tag{22}$$

where one needs to define two more parameters for each quark flavor:

$$\mathcal{I}_c^i = \int \frac{d^3p}{(2\pi)^3}\frac{1}{p}[f^g + f^{q^i} + f^g(f^{q^i} - f^{\bar{q}^i})],$$

$$\bar{\mathcal{I}}_c^i = \int \frac{d^3p}{(2\pi)^3}\frac{1}{p}[f^g + f^{\bar{q}^i} + f^g(f^{\bar{q}^i} - f^{q^i})]. \tag{23}$$

- In the collinear limit, the splitting processes

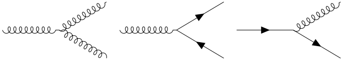

factorizes. The rest part of the diagrams can be hence integrated out to define the splitting rate $dI_{a\to bc}/dxdt$ for a splitting process $a \to bc$.

- The $1 \leftrightarrow 2$ kernel takes the form

$$C^a_{1\leftrightarrow 2} = \int_0^1 dx \sum_{b,c} \left[\frac{1}{x^3} \frac{\nu_c}{\nu_a} C^c_{ab}(\boldsymbol{p}/x; \boldsymbol{p}, \boldsymbol{p}(1-x)/x) - \frac{1}{2} C^a_{bc}(\boldsymbol{p}; x\boldsymbol{p}, (1-x)\boldsymbol{p}) \right],$$

where ν_a is the number of spin times color degrees of freedom for parton a: $\nu_a = 2N_c$ for q or $\bar{q}$ and $\nu_a = 2(N_c^2 - 1)$ for g, and

$$C^a_{bc}(\boldsymbol{p}; x\boldsymbol{p}, (1-x)\boldsymbol{p}) \equiv \frac{dI_{a\to bc}(p)}{dxdt} \mathcal{F}^a_{bc}(\boldsymbol{p}; x\boldsymbol{p}, (1-x)\boldsymbol{p}) \tag{24}$$

with

$$\mathcal{F}^a_{bc}(\boldsymbol{p}; \boldsymbol{l}, \boldsymbol{k}) = f^a_{\boldsymbol{p}}(1 + \epsilon_b f^b_{\boldsymbol{l}})(1 + \epsilon_c f^c_{\boldsymbol{k}}) - f^b_{\boldsymbol{l}} f^c_{\boldsymbol{k}}(1 + \epsilon_a f^a_{\boldsymbol{p}}). \tag{25}$$

Here, x is the momentum fraction carried by particle b for the process $a \to bc$, $\boldsymbol{l} \equiv x$p and $\boldsymbol{k} \equiv (1-x)$p.

- Why are $2 \leftrightarrow 2$ and $1 \leftrightarrow 2$ kernels of the same order?

For example, for the $2 \leftrightarrow 3$ process, one has splitting rate

$$\frac{dI_{a\to bc}(p)}{dxdt} \propto \int d^3p f_p(1+f_p) \underbrace{\sigma_{el}}_{2\leftrightarrow 2} \underbrace{\alpha_s P_{a\to bc}(z)}_{\text{collinear splitting}}$$

$$\propto Q^3 \frac{\alpha_s^2}{m_D^2} \alpha_s P_{a\to bc}(z) \propto \alpha_s^2 Q P_{a\to bc}(z)$$

with $P_{a\to bc}(z)$ the splitting function, $m_D^2 \sim \alpha_s Q^2$ and Q typical momentum.

- We use the splitting kernel with the LPM effect:

$$\frac{dI_{g\to gg}(p)}{dxdt} = \frac{\alpha_s N_c}{\pi} \frac{(1-x+x^2)^{5/2}}{(x-x^2)^{3/2}} \sqrt{\frac{\hat{q}_A}{p}},$$

$$\frac{dI_{g\to q\bar{q}}(p)}{dxdt} = \frac{\alpha_s}{4\pi}[x^2+(1-x)^2]\left[\frac{\frac{C_F}{C_A}-x(1-x)}{x(1-x)}\right]^{\frac{1}{2}} \sqrt{\frac{\hat{q}_A}{p}},$$

$$\frac{dI_{q\to gq}(p)}{dxdt} = \frac{dI_{\bar{q}\to g\bar{q}}(p)}{dxdt} = \frac{\alpha_s C_F}{2\pi} \frac{1+(1-x)^2}{x}\left[\frac{1-x+\frac{C_F}{C_A}x^2}{x(1-x)}\right]^{\frac{1}{2}} \sqrt{\frac{\hat{q}_A}{p}},$$

$$\frac{dI_{q\to qg}(p)}{dxdt} = \frac{dI_{\bar{q}\to \bar{q}g}(p)}{dxdt} = \frac{\alpha_s C_F}{2\pi} \frac{1+x^2}{1-x}\left[\frac{x+\frac{C_F}{C_A}(1-x)^2}{x(1-x)}\right]^{\frac{1}{2}} \sqrt{\frac{\hat{q}_A}{p}}.$$

- The $2 \leftrightarrow 2$ kernel conserves
  1. the net quark number for each quark flavor
  2. the total energy
  3. the total parton number
- The $1 \leftrightarrow 2$ kernel conserves
  1. the net quark number for each quark flavor
  2. the total energy
- The BEDA conserves
  1. the net quark number for each quark flavor
  2. the total energy

Besides, the set of BEDA is invariant under $q^i \leftrightarrow \bar{q}^i$ and respects flavor symmetries (for massless quarks).

3.1 Partons freed from nulcear PDFs

- In the limit $\sqrt{s_{NN}} \gg Q_s \gg \Lambda_{QCD}$, the following picture emerges:

1. The valence quarks and large-x partons mostly pass through each other, carrying away a large portion of collision energy (and the Baryon numbers)

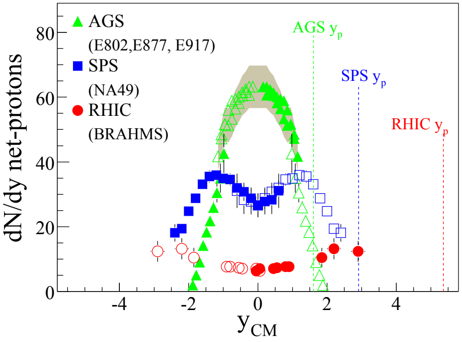

I. G. Bearden *et al.* [BRAHMS], Phys. Rev. Lett. **93**, 102301 (2004) [arXiv:nucl-ex/0312023 [nucl-ex]].

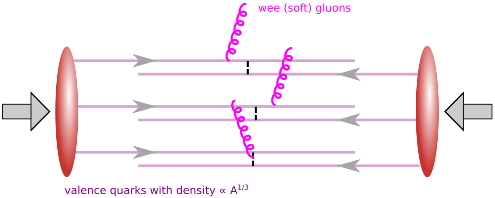

Bjorken, Lect. Notes Phys. **56**, 93 (1976).

2 Longitudinal boost-invariance: "wee" partons fill a central plateau.

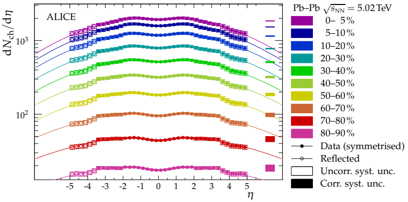

J. Adam *et al.* [ALICE], Phys. Lett. B **772**, 567-577 (2017) [arXiv:1612.08966 [nucl-ex]].

Because soft gluon spectrum $\propto \omega \frac{dI}{d\omega} = \frac{dI}{d\eta} \sim \alpha_s$. In CGC, $\omega \sim Q_s$.

- Accordingly, our initial distributions:

$$f(t=0) = f_0\theta(Q - |\vec{p}|), \qquad F(t=0) = F_0 = 0, \qquad \bar{F}(t=0) = \bar{F}_0 = 0$$

where Q can be viewed as the saturation momentum, and

$$f = f^g, \qquad F = f^q, \qquad \bar{F} = f^{\bar{q}}$$

- Let us study thermalization and the production of three flavors of massless quarks ($N_f = 3$).

- Obviously, all the quarks and antiquarks should have the same distriubiton all the time as the BEDA is invariant under $q^i \leftrightarrow \bar{q}^i$ and respects flavor symmetries.

- We first study spatially homogeneous systems as in lattice QCD.

S. Barrera Cabodevila, C. A. Salgado and BW, Phys. Lett. B **834** (2022), 137491 [arXiv:2206.12376 [hep-ph]]; JHEP **06** (2024), 145 [arXiv:2311.07450 [hep-ph]].

- The $1 \leftrightarrow 2$ kernel becomes dominant at small p:

$$C^{g}_{1\leftrightarrow 2} \approx \frac{\alpha_s}{2\pi}\sqrt{\frac{\hat{q}_A}{p}}\int \frac{dx}{x^4}\left[2N_c\mathcal{F}^{g}_{gg} + \sum_{i=1}^{N_f}\left(\mathcal{F}^{q^i}_{gq^i} + \mathcal{F}^{\bar{q}^i}_{g\bar{q}^i}\right)\right]\left(\frac{\boldsymbol{p}}{x};\boldsymbol{p},\frac{1-x}{x}\boldsymbol{p}\right)$$

$$\approx \frac{\alpha_s N_c}{\pi} I_a \sqrt{\frac{\hat{q}_A}{p}}\frac{1}{p^3}\left(1 - \frac{pf^g}{T_*}\right),$$

$$C^{q^i}_{1\leftrightarrow 2} \approx \frac{\alpha_s C_F}{2\pi}\sqrt{\frac{\hat{q}_F}{p}}\int \frac{dx}{x^3}\left[\mathcal{F}^{q^i}_{q^i g} + \mathcal{F}^{g}_{q^i\bar{q}^i}\right]\left(\frac{\boldsymbol{p}}{x};\boldsymbol{p},\frac{1-x}{x}\boldsymbol{p}\right)$$

$$\approx \alpha_s C_F \pi(\mathcal{I}^i_c + \bar{\mathcal{I}}^i_c)\sqrt{\frac{\hat{q}_F}{p}}\frac{1}{p^2}\left(\frac{1}{e^{-\frac{\mu^i_*}{T_*}}+1} - f^{q^i}\right),$$

$$C^{\bar{q}^i}_{1\leftrightarrow 2} \approx \alpha_s C_F \pi(\mathcal{I}^i_c + \bar{\mathcal{I}}^i_c)\sqrt{\frac{\hat{q}_F}{p}}\frac{1}{p^2}\left(\frac{1}{e^{\frac{\mu^i_*}{T_*}}+1} - f^{\bar{q}^i}\right)$$

- It dictates that at any time one always has for $p \to 0$

$$pf^g \to T_*, \qquad f^{q^i} \to \frac{1}{e^{-\frac{\mu_*^i}{T_*}} + 1}, \qquad f^{\bar{q}^i} \to \frac{1}{e^{\frac{\mu_*^i}{T_*}} + 1}.$$

- That is, the soft sector $p \to 0$ is the same as that with temperatore given by The effective temperature

$$T_*(t) \equiv \frac{\hat{q}_A}{\alpha_s N_c \mathcal{L} m_D^2}$$

and the net quark chemical potential for flavor i given by

$$\mu_*^i = T_* \ln \frac{\mathcal{I}_c^i}{\bar{\mathcal{I}}_c^i}.$$

- In the case $f^{q^i} = f^{\bar{q}^i}$, $\mu_*^i = 0$. The evolution is characterized by $\hat{q}$ and m_D^2.

3.2.1 Initially over-populated systems

• Would a (transient) **Bose-Einstein Condensate (BEC) of gluons** form? We find that including $1 \leftrightarrow 2$ kernel removes the accumulation of gluons at $p = 0$, which was previously interpreted as a BEC:

1. Without the $1 \leftrightarrow 2$ kernel, we observed an accumulation of gluons at $p = 0$ with the number density proportional to $(\lim_{p \to 0} pf^g - T_*) \neq 0$. This is easily understood from

$$\dot{f}^a = \frac{1}{p^2}(p^2 J^a)' + \mathcal{S}_a$$

with

$$\frac{1}{p^2}(p^2 J^a)' \equiv \frac{1}{4}\frac{\hat{q}_a}{p^2}\left[p^2\left(f^{a\prime} + \frac{1}{T_*}f^a(1+\epsilon_a f^a)\right)\right]'.$$

J. P. Blaizot, BW and L. Yan, Nucl. Phys. A **930** (2014), 139-162 [arXiv:1402.5049 [hep-ph]].

2. Including the $1 \leftrightarrow 2$ kernel modifies the distributions at small p such that $(\lim_{p \to 0} pf^g - T_*) = 0$. Therefore, No BEC.

- Parametric estimates for $f_0 \gg 1$: thermalization proceeds in two stages

1. Soft gluon radiation and overheating: $0 \ll Qt \ll (\alpha_s f_0)^{-2}$

$$T_* \sim f_0 Q \gg T \sim f_0^{\frac{1}{4}} Q, m_D^2 \sim \alpha_s f_0 Q^2, \quad \hat{q} \sim \alpha_s^2 f_0^2 Q^3$$

2. Momentum broadening and cooling: $(\alpha_s f_0)^{-2} \ll Qt \ll \alpha_s^{-\frac{7}{4}} (\alpha_s f_0)^{-\frac{1}{4}}$
   At this stage, the typical momentum of gluons increases due to multiple scattering. So, the gluon number has to decrease due to energy conservation:

$$p^2 \sim \hat{q} t \sim \alpha_s^2 n_g^2 t / p^3, \qquad \epsilon \sim f_0 Q^4 \sim n_g p$$

   yields

$$n_g \sim \frac{(\alpha_s f_0)^{\frac{5}{7}}}{\alpha_s} \frac{Q^3}{(Qt)^{\frac{1}{7}}}, \qquad p \sim (\alpha_s f_0)^{\frac{2}{7}} (Qt)^{\frac{1}{7}} Q, \qquad f \sim \frac{(\alpha_s f_0)^{-\frac{1}{7}}}{\alpha_s} \frac{1}{(Qt)^{\frac{4}{7}}},$$

$$\hat{q} \sim (\alpha_s f_0)^{\frac{4}{7}} \frac{Q^3}{(Qt)^{\frac{5}{7}}}, \qquad m_D^2 \sim (\alpha_s f_0)^{\frac{3}{7}} \frac{Q^2}{(Qt)^{\frac{2}{7}}}, \qquad T_* \sim \frac{(\alpha_s f_0)^{\frac{1}{7}}}{\alpha_s} \frac{Q}{(Qt)^{\frac{3}{7}}} \sim pf.$$

At $Qt \sim \alpha_s^{-\frac{7}{4}} (\alpha_s f_0)^{-\frac{1}{4}}$, all the above quantities approach their final equilibrium values and full thermalization is established around this time.

- The scaling behavior is universal

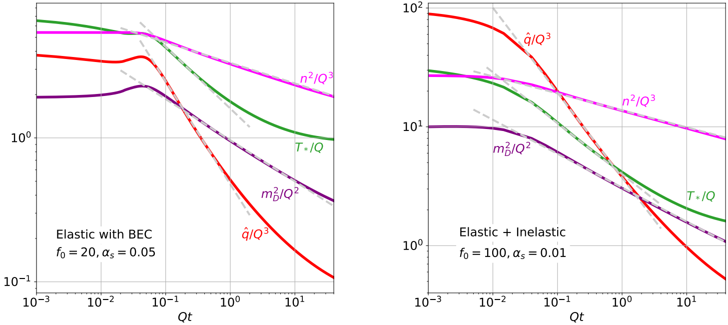

S. Barrera Cabodevila, C. A. Salgado and BW, Phys. Lett. B **834** (2022), 137491 [arXiv:2206.12376 [hep-ph]].

- It is also referred to as the non-thermal fixed point.

e.g., S. Schlichting, Phys. Rev. D **86** (2012), 065008 [arXiv:1207.1450 [hep-ph]].

- Quark production:

$$n_q \sim \begin{cases} \alpha_s^2 f_0^2 Q^4 t & \text{during } 0 \ll Qt \ll (\alpha_s f_0)^{-2} \\ (\alpha_s f_0)^{\frac{6}{7}} (Qt)^{\frac{3}{7}} Q^3 & \text{during } (\alpha_s f_0)^{-2} \ll Qt \ll \alpha_s^{-\frac{7}{4}} (\alpha_s f_0)^{-\frac{1}{4}} \end{cases}$$

- Quark production does not change the universal scaling behavior

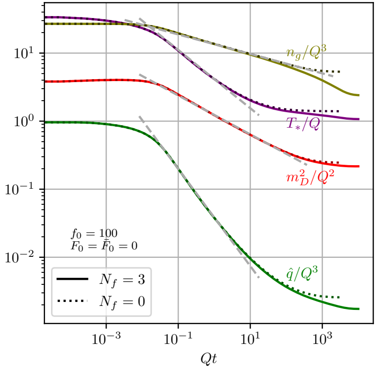

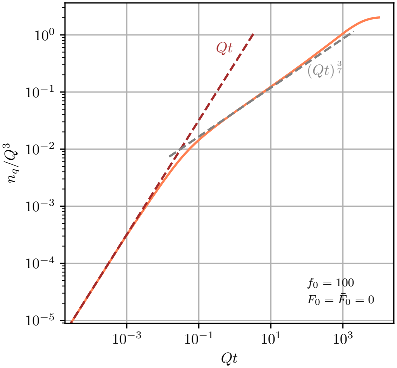

- Scaling behavior is related to the following self-similar solutions:

$$f = (Qt)^{-\frac{3}{7}} \frac{Q}{p} D_s(p/\bar{p}) \equiv (Qt)^{-\frac{4}{7}} f_s(\tilde{p}), \qquad F = F_s(\tilde{p})$$

with $\tilde{p} \equiv (Qt)^{-\frac{1}{7}} p/Q$.

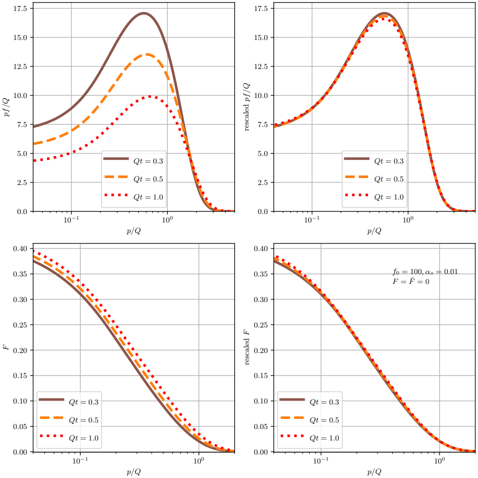

• Gluons undergo the top-down thermalization: at the late stage of the evolution, gluons thermalize at higher temperature first and gradually cool down to the thermal equilibrium temperature by producing q and $\bar{q}$

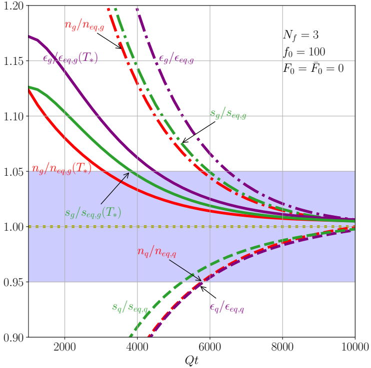

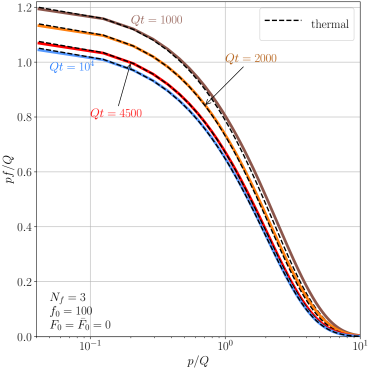

• This is due to the fact that quarks are produced more slowly than gluons:

$$\frac{dI_{a\to ga}(p)}{dxdt} \sim \frac{\alpha_s N_c}{\pi} \frac{1}{x^{3/2}} \sqrt{\frac{\hat{q}_a}{p}} \text{ vs } \frac{dI_{g\to q\bar{q}}(p)}{dxdt} = \frac{\alpha_s}{4\pi} \left[\frac{C_F}{C_A}\right]^{\frac{1}{2}} \frac{1}{x^{1/2}} \sqrt{\frac{\hat{q}_A}{p}}$$

3.2.2 Initially under-populated systems

- Parametric estimates for $f_0 \ll 1$: thermalization proceeds in three stages

1. Overheating in the soft sector: $0 \ll Qt \ll \alpha_s^{-2} f_0$
   During this stage, the properties of the system are dominated by hard gluons with $p \sim Q$, yielding

$$n_g \sim n_{h,g} \sim f_0 Q^3, \quad m_D^2 \sim \alpha_s f_0 Q^2, \quad \hat{q} \sim \alpha_s^2 f_0 Q^3, \quad T_* \sim Q \gg T \sim f_0^{\frac{1}{4}} Q$$

2. Cooling and overcooling in the soft sector: $\alpha_s^{-2} f_0 \ll Qt \ll \alpha_s^{-2} f_0^{-\frac{1}{3}}$
   $\hat{q}$ is dominated by hard gluons while m_D^2 is dominated by soft gluons, yielding respectively

$$\hat{q} \sim \alpha_s^2 f_0 Q^3, m_D^2 \sim \alpha_s^{\frac{3}{2}} f_0^{\frac{3}{4}} (Qt)^{\frac{1}{4}} Q^2 \Rightarrow T_* \sim \alpha_s^{-\frac{1}{2}} f_0^{\frac{1}{4}} (Qt)^{-\frac{1}{4}} Q$$

   The system sets up the stage for thermalization.

3. Reheating and mini-jet quenching: $\alpha_s^{-2} f_0^{-\frac{1}{3}} \ll Qt \ll \alpha_s^{-2} f_0^{-\frac{3}{8}}$
   Soft gluons always have enough time to establish a thermal bath. Both $\hat{q}$ and m_D^2 are dominated by soft gluons. Hard partons are quenched, heating up the soft thermal bath, undergoing the bottom-up thermalization with $T_* \sim \alpha_s^4 f_0 (Qt)^2 Q, m_D^2 \sim \alpha_s^9 f_0^2 (Qt)^4 Q^2, \hat{q} \sim \alpha_s^{14} f_0^3 (Qt)^6 Q^3$

• In pure gluon systems ($N_f = 0$): numerical results qualitatively agree with the parametric estimates for $f_0 = 0.01$.

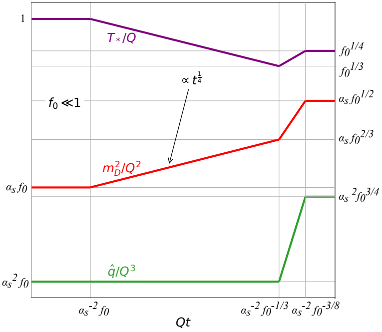

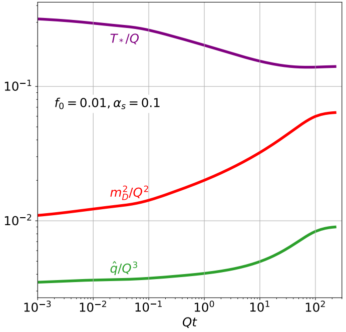

- Parametric estimates for quark production:

$$n_q \sim \begin{cases} \alpha_s^2 f_0^{\frac{3}{2}} Q^4 t & \text{at } Qt \lesssim \alpha_s^{-2} \\ \alpha_s^3 f_0^{\frac{3}{2}} (Qt)^{\frac{3}{2}} Q^3 & \text{at } \alpha_s^{-2} \lesssim Qt \lesssim \alpha_s^{-2} f_0^{-\frac{1}{3}} \\ \alpha_s^{12} f_0^3 (Qt)^6 Q^3 & \text{at } \alpha_s^{-2} f_0^{-\frac{1}{3}} \lesssim Qt \lesssim \alpha_s^{-2} f_0^{-\frac{3}{8}} \end{cases} .$$

- Numerical result for $N_f = 3$:

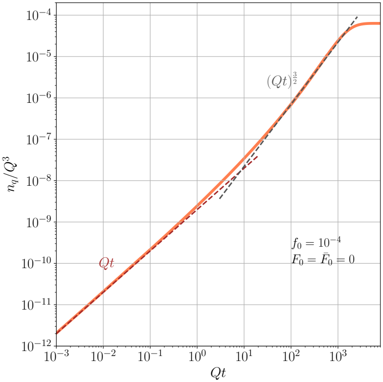

• Including quark production does not spoils the three-stage thermalizaiton. However, for $N_f = 3$, one needs to go to even smaller f_0 to see the bottom-up thermalization.

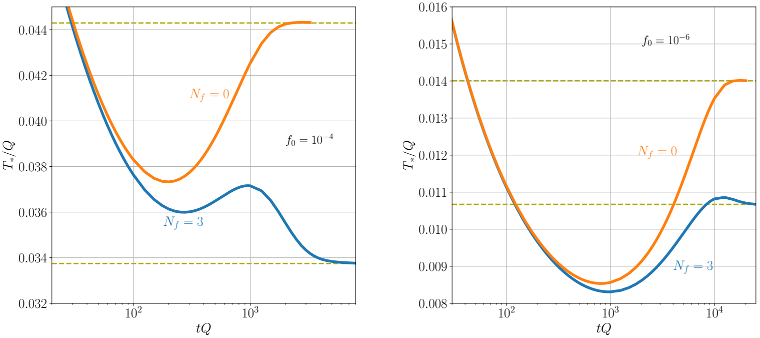

• For $f_0 \geq 10^{-4}$, we find that gluons all undergo the top-down thermalization near the end of the thermalization process.

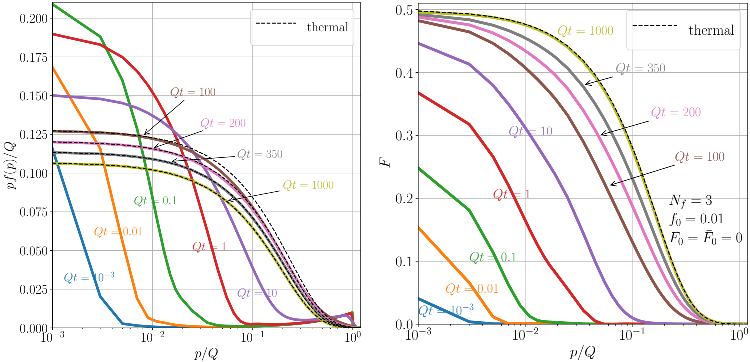

3.3 Longitudinally boost-invariant systems

• At $\tau = t_0 \sim 1/Q_s$, the saturated gluons, referred to as "hard", are freed from the nuclear wave functions with

$$p \sim Q_s, \qquad \text{number density } n_h \sim \frac{1}{\alpha_s}$$

• For $t > 1/Q_s$, the thermalization process can be described by kinetic theory.

At $z = 0$, the BEDA takes the form

$$\left(\partial_t - \frac{p_z}{t}\partial_{p_z}\right) f^a(p_T, p_z, t) = C^a_{2\leftrightarrow 2} + C^a_{1\leftrightarrow 2}.$$

Baier, Mueller, Schiff and Son, Phys. Lett. B **502**, 51 (2001) [hep-ph/0009237].

• The effects of expansion: Without any scattering, one has the free-streaming solution $f^a(p_T, p_z, t) = f^a(p_T, p_z t/t_0, t_0)$. That is, the typical value of $p_z \propto 1/t$.

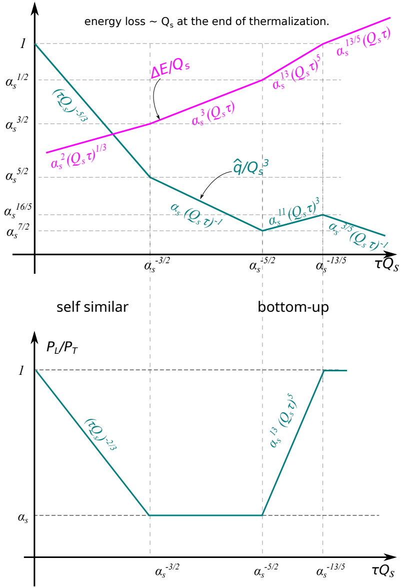

Three stages of thermalization:

1. $\alpha_s^{-\frac{3}{2}} \gtrsim \tau Q_s \gtrsim 1$
   The system is over-populated with $f \gtrsim 1$. $\hat{q}$ and m_D^2 are dominated by hard gluons. The interplay between momentum broadening and expansion leads to the self-similar behavior.
2. $\alpha_s^{-\frac{5}{2}} \gtrsim \tau Q_s \gtrsim \alpha_s^{-\frac{3}{2}}$
   $\hat{q}$ is dominated by hard gluons while m_D^2 is dominated by soft gluons. The system sets up the stage for thermalization.
3. $\alpha_s^{-\frac{13}{5}} \gtrsim \tau Q_s \gtrsim \alpha_s^{-\frac{5}{2}}$
   Soft gluons always have enough time to establish a thermal bath. Both $\hat{q}$ and m_D^2 are dominated by soft gluons. Hard partons are quenched, heating up the soft thermal bath, undergoing the bottom-up thermalization.

- Numerical confirmations using EKT: hydrodynamization at intermediate coupling

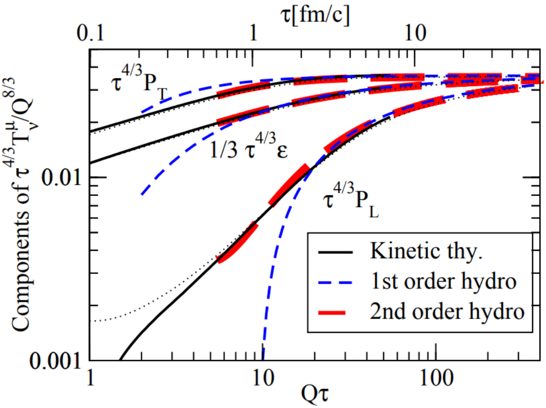

A. Kurkela and Y. Zhu, Phys. Rev. Lett. **115** (2015) no.18, 182301 [arXiv:1506.06647 [hep-ph]].

4 Perspective: flow in small systems

• Preequilibrium dynamics is intriguing although it may not play a significant role in phenomenology in heavy-ion collisions.

• It is expected to be important for phenomenology in small systems.

• Here, I illustrate this point using kinetic theory in relaxation time approximation (RTA):

$$\partial_\tau f + \vec{v}_\perp \cdot \partial_{\vec{x}_\perp} f - \frac{p^z}{\tau} \partial_{p^z} f = -C[f] \,.$$

with

$$-C[F] = -\gamma \varepsilon^{1/4}(x)[-v_\mu u^\mu](F - F_{\rm iso})$$

where $F_{\rm iso}$ is the isotropic distribution in the rest frame u^μ. In RTA, physics depends on only one dimensionless parameter:

$$\text{Opacity: } \hat{\gamma} = \gamma R^{\frac{3}{4}} (\varepsilon_0 \tau_0)^{\frac{1}{4}} = R/l_{mfp}$$

with l_{mfp} mean free path.

Kurkela, Wiedemann and BW, Phys. Lett. B **783**, 274 (2018), [arXiv:1803.02072].

- From mode-mode coupling due to one final-state scattering

$$\frac{dE_\perp}{d\eta d\phi} = \frac{1}{2\pi}\frac{dE_\perp}{d\eta}\Big|_{\hat\gamma=0,\epsilon_n=0} \Big\{ 1 - 0.210\,\hat\gamma - \underbrace{0.212\,\hat\gamma\epsilon_2}_{v_2} 2\cos(2\phi - 2\psi_2)$$

$$-\underbrace{0.140\,\hat\gamma\epsilon_3}_{v_3} 2\cos(3\phi - 3\psi_3)$$

$$+\underbrace{0.063\,\hat\gamma\epsilon_2^2}_{v_4} 2\cos(4\phi - 4\psi_2) + 0.015\,\hat\gamma\epsilon_2^2$$

$$+\underbrace{0.112\,\hat\gamma\epsilon_3^2}_{v_6} 2\cos(6\phi - 6\psi_3) + 0.043\,\hat\gamma\epsilon_3^2$$

$$+\underbrace{0.088\,\hat\gamma\epsilon_2\epsilon_3}_{v_5} 2\cos(5\phi - 3\psi_3 - 2\psi_2) \Big\}$$

with ϵ_n spatial eccentricities.

- Flow in small and/or dilute limit

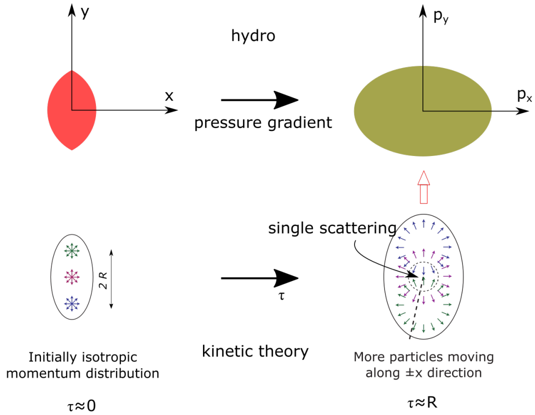

See also: Borghini & Gombeaud, Eur. Phys. J. C **71** (2011) 1612; He, Edmonds, Lin, Liu, Molnar & Wang, Phys. Lett. B **753** (2016) 506.

• Kinetic theory bridges nonhydrodynamic (single hit) and hydrodynamic contributions.

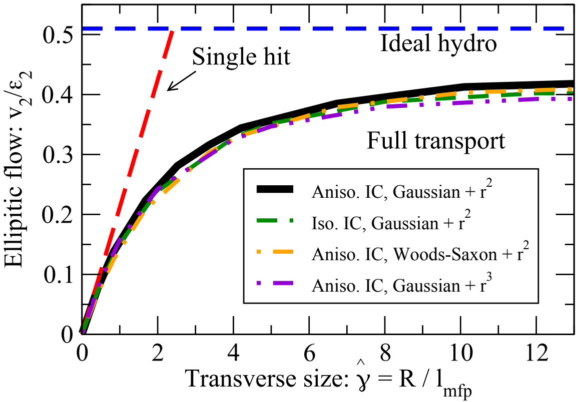

A. Kurkela, U. A. Wiedemann and BW, Eur. Phys. J. C **79**, no. 11, 965 (2019) [arXiv:1905.05139 [hep-ph]].

- One may probe more preequilibrium dynamics in smaller systems:

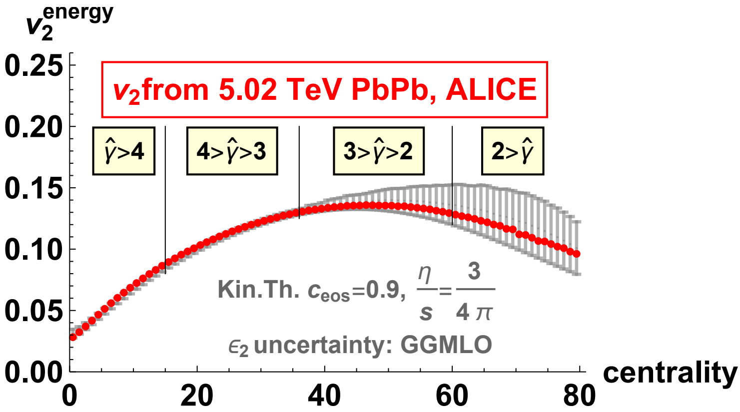

- Commonalities with bottom-up thermalization:
  - Early-time attractor
  - Late-time (hydro) attractor

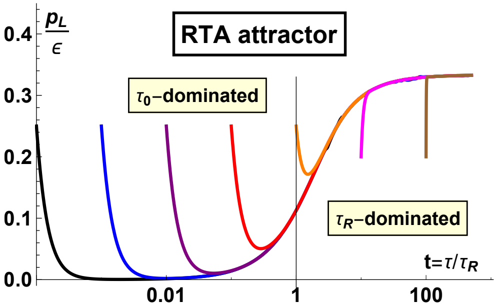

Definition: an attractor is the particular solution to which arbitrary initial conditions within the basin of attraction relax at sufficiently late times.

Kurkela, van der Schee, Wiedemann and BW, Phys. Rev. Lett. **124**, 102301 (2020) [arXiv:1907.08101 [hep-ph]]..

- In Israel-Stewart hydrodynamics and AdS/CFT:

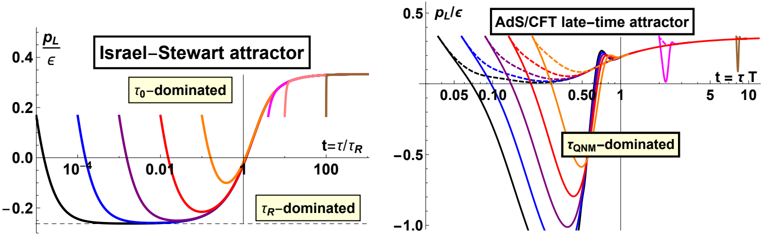

Kurkela, van der Schee, Wiedemann and BW, Phys. Rev. Lett. **124**, 102301 (2020) [arXiv:1907.08101 [hep-ph]]..

They have the same late-time attractor but the three theories are radically different especially in early times!

• Concluding remark: In smaller collision systems, one would expect larger contributions from nonhydrodynamic dynamics.

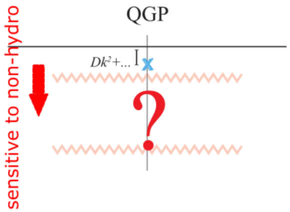

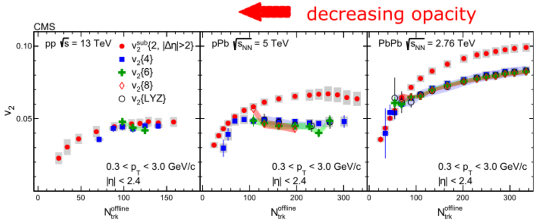

More to be done using EKT or BEDA!